Arctic sea-ice variability revisited

Julienne STROEVE,[1] Allan FREI,[2,3] James McCREIGHT,[1] Debjani GHATAK[3]

[1]*National Snow and Ice Data Center, Cooperative Institute for Research in Environmental Sciences, Campus Box 449, University of Colorado, Boulder, CO 80309-0449 USA*
E-mail: stroeve@kryos.colorado.edu
[2]*Hunter College Department of Geography, 695 Park Avenue, New York, NY 10021, USA*
[3]*Program in Earth and Environmental Sciences, City University of New York, 365 5th Avenue, New York, NY 10016, USA*

ABSTRACT. This paper explores spatial and temporal relationships between variations in Arctic sea-ice concentration (summer and winter) and near-surface atmospheric temperature and atmospheric pressure using multivariate statistical techniques. Trend, empirical orthogonal function (EOF) and singular value decomposition (SVD) analyses are used to identify spatial patterns associated with covariances and correlations between these fields. Results show that (1) in winter, the Arctic Oscillation still explains most of the variability in sea-ice concentration from 1979 to 2006; and (2) in summer, a decreasing sea-ice trend centered in the Pacific sector of the Arctic basin is clearly correlated to an Arctic-wide air temperature warming trend. These results demonstrate the applicability of multivariate methods, and in particular SVD analysis, which has not been used in earlier studies for assessment of changes in the Arctic sea-ice cover. Results are consistent with the interpretation that a warming signal has now emerged from the noise in the Arctic sea-ice record during summer. Our analysis indicates that such a signal may also be forthcoming during winter.

1. INTRODUCTION

The latest report released by the Intergovernmental Panel on Climate Change (IPCC; Solomon and others, 2007) concludes that anthropogenic warming is largely responsible for rising temperatures over the last 50 years, and will likely lead to accelerated warming, resulting in significantly decreased sea-ice cover in the Arctic. Presently, the observational record of Arctic sea ice shows the areal extent of sea ice is rapidly declining, in agreement with climate model simulations that all show ice loss during the observational record under various greenhouse gas (GHG) scenarios. Negative trends in ice extent (defined as total area with at least 15% ice concentration), while largest at the end of the summer melt season in September ($-10.7\%\,(10\,\mathrm{a})^{-1}$ from 1979 to 2007), now encompass all months. Moreover, the rate at which the sea ice is disappearing is outpacing even the most pessimistic climate-model projections. Recent comparisons between the observational record and climate model output from the IPCC Fourth Assessment Report reveal that current summer ice conditions in the Arctic are on average 30 years ahead of model predictions (i.e. models are underestimating the rate of ice loss), leading to speculation that the transition to a seasonally ice-free Arctic may happen sooner than the 2050–2100 time frame suggested by the model simulations (Stroeve and others, 2007).

How do we explain these rapid ice losses? It is tempting to implicate rising air temperatures from GHG loading. Many studies have suggested increased concentrations of GHGs are playing an increasingly strong role in the loss of the Arctic ice cover (e.g. Zhang and Walsh, 2006; Stroeve and others, 2007). However, several other studies have also linked the loss of sea ice and other high-latitude changes to changes in atmospheric circulation patterns such as the Arctic Oscillation (AO) (e.g. Deser and others, 2000; Rigor and others, 2002; Rigor and Wallace, 2004; Liu and others, 2007). There is evidence that the strongly positive phase of the winter AO in the early to mid-1990s led to the export of thick, multi-year ice out of the Arctic basin, leaving behind thinner ice that is more easily melted (Rigor and Wallace, 2004). Support for this view comes from the tracking of the age of the ice in the Arctic using satellite data which suggest that Arctic ice is younger now than it was in the 1980s (Fowler and others, 2004). Rigor and Wallace (2004) estimate that the combined winter and summer AO indices can explain less than 20% of the variance in summer sea-ice extent in the western Arctic, where most of the recent reduction in sea-ice cover has occurred. Maslanik and others (2007a) argue that atmospheric circulation patterns other than the AO have also contributed. A separate analysis of the combined effects of winds, radiative fluxes and advected heat shows that atmospheric forcing can account for about one-half of the total variance in summer sea-ice extent in the western Arctic (Francis and Hunter, 2006). A more recent analysis (Liu and others, 2007) suggests that variations in the AO, acting in combination with variations in the Aleutian low, can explain a large portion of recent land surface changes that were previously attributed to a warming trend.

In short, the causes of the now Arctic-wide sea-ice decline are far from resolved. It is logical to surmise that part of the sea-ice decline represents a growing radiative forcing from GHG loading, while other patterns of sea-ice concentration variability are still driven to large extent by Arctic atmospheric circulation patterns including the AO. As GHG loadings mount, a signal of sea-ice decline with atmospheric warming may begin to decouple from the patterns of sea-ice variability controlled by circulation patterns. The goal of this paper is to expand upon previous multivariate analyses of sea-ice variations such as that by Deser and others (2000) using the most up-to-date satellite observations of Arctic sea ice (through summer 2006). We also introduce singular value decomposition (SVD) analysis to this multivariate problem as a tool to help distinguish different signals (e.g. trends associated with warming vs periodic variations associated with the AO) in the sea-ice record and to

https://doi.org/10.3189/172756408784700699 Published online by Cambridge University Press

determine their relevant spatial and temporal patterns. These methods provide insight into the most important signals present in the sea-ice record, and into sea-ice variability relationships with other fields. Our analysis focuses on the months of climatological minimum (September) and maximum (March) Arctic ice cover.

2. DATA AND METHODOLOGY

In this study, gridded fields of sea-ice concentration (IC) derived from a series of successive multichannel passive microwave satellite observations since the late 1970s are used. The fraction of sea ice occupying a gridcell is derived using the Bootstrap algorithm (J.C. Comiso, http://www.nsidc.org/data/nsidc-0079.html), and monthly mean fields are computed for March and September using a 15% IC cutoff, i.e. pixels with ICs less than 15% are assumed to be ice-free. These data are available from the US National Snow and Ice Data Center (http://nsidc.org) and span the period 1979–2006. In order to reduce the size of computed correlation matrices, the data have been regridded to a 100 km Equal-Area Scalable Earth Grid (EASE-Grid) (M.J. Brodzick and K.W. Knowles, http://www.ncgia.ucsb.edu/globalgrids/abstracts/Brodzick.htm).

Air temperature at the 925 hPa level (T_{925}) and sea-level pressure (SLP) from the US National Centers for Environmental Prediction(NCEP)/US National Center for Atmospheric Research (NCAR) re-analysis (Kalnay and others, 1996) are examined in conjunction with the sea-ice record. Here we use 925 hPa, rather than surface air temperature (SAT) fields, since the 925 hPa fields are more constrained by observations than the SAT fields. SLP and T_{925} fields are expressed as monthly, seasonal and annual means. In the multivariate analysis, T_{925} from 90N to 55N (50N) are used with September (March) IC. For SLP, the spatial domain extends from 90N to 20N. In empirical orthogonal function (EOF) and SVD analysis, these fields are given a standard cosine-of-latitude weighting to account for the change of gridcell spacing/area with latitude (i.e. greater clustering of values near the pole) (e.g. Deser and others, 2000; Huth, 2006).

We show results from three types of analyses: trend, EOF and SVD. The non-parametric Mann–Kendall test (Mann, 1945) is used to robustly identify regions of statistically significant (95% confidence) trends in each variable. Only significant trends are reported, and trends are defined as the slope of the least-squares fitted line.

Both EOF and SVD provide a decomposition of the original space–time fields, indicating primary temporal signals and associated spatial patterns (or 'modes') present in the original fields. EOF analysis decomposes the covariance matrix of a single field into bi-orthogonal modes or pairs of spatial patterns (EOFs) and time series (or principal components (PCs)), and reveals the fraction of the total variance in the field explained by each mode. In this paper, each EOF is represented by a map of the linear regression coefficients of the anomaly time series at each gridpoint onto the PC time series, similar to what is done by Deser and others (2000). While not a true EOF, the spatial patterns are qualitatively similar to the EOF patterns and the regression provides meaningful units.

SVD analysis performs a similar decomposition of the cross-correlation or cross-covariance matrix between two fields, yielding modes or pairs of spatial patterns. Time components (TCs) for each field, in this case, are obtained via projection of the data onto the spatial patterns obtained for each field. SVD identifies the modes which maximize the mean-squared temporal covariance of the two fields. We perform SVD using the correlation matrix since the two covarying fields do not share units. Although SVD analysis has not been used widely in meteorology and to our knowledge has never been used in sea-ice studies, it can be useful for isolating signals (modes of variance) in two fields that are related to each other. However, caution is needed in interpretation of the SVD results to ensure that the joint signals identified are actually significant (e.g. Hu, 1997). Toward that end, we produce *heterogeneous correlation* (HC) *maps* (Bretherton and others, 1992), which show the correlation coefficients between the time series at each gridpoint of one field and the TC time series of the other field. These are necessary because, while the SVD analysis identifies signals that explain the maximum variance between the two fields, HC maps allow one to evaluate the statistical significance of the mutual variance in the usual ways that correlation maps are evaluated. When no coherent structure is present in one or both HC plots, we assume no coherent relationship between the two fields is represented by that mode of the SVD analysis (e.g. Rajagopalan and others, 2000). However, if structured correlation is found in both HC plots, the spatial patterns of the correlation values indicate the regions over which the two fields are related. In this study, HC maps are computed using the non-parametric Spearman correlation coefficient (ρ). Only coefficients with at least 95% probability of significance are reported. The results are consistent with those using the parametric Pearson's as well as the non-parametric Kendall's tau results (not shown).

Because of page limitations we only show figures related to the first EOF and SVD modes in section 3. Other modes are discussed in the text. The relevance of these results to the questions of climate change detection, and of distinguishing cause from effect, is discussed in section 4.

3. RESULTS

3.1. Trends

Figure 1 shows September and March IC trends and annual T_{925} trends at gridpoints with significant (95% confidence) trends. In September (Fig. 1a), statistically significant negative trends in sea-ice concentration occur in the Beaufort, Chukchi, East Siberian, Laptev and East Greenland seas. This is consistent with earlier studies that reported large ice losses in these regions during the last 5 years (e.g. Serreze and others, 2003; Stroeve and others, 2005). The largest negative sea-ice trends occur in the Beaufort and Chukchi seas at rates of around –30% IC $(10\,a)^{-1}$. Negative trends in IC are also observed in the East Greenland Sea (–10 to –15% IC $(10\,a)^{-1}$). In 2002, sea ice disappeared for the first time during the satellite record from the Greenland shelf. The situation was repeated in 2003, and although there has been some ice in the East Greenland Sea since 2003, the ice coverage remains anomalously low.

The March IC trend map shows areas of both loss and gain (Fig. 1b). The scattered areas of IC loss occur in the marginal ice zone (MIZ), over both the Atlantic and Pacific sectors, as well as south of Bering Strait where the trends are mixed. Trends along the MIZ range from –10 to –25% IC $(10\,a)^{-1}$,

https://doi.org/10.3189/172756408784700699 Published online by Cambridge University Press

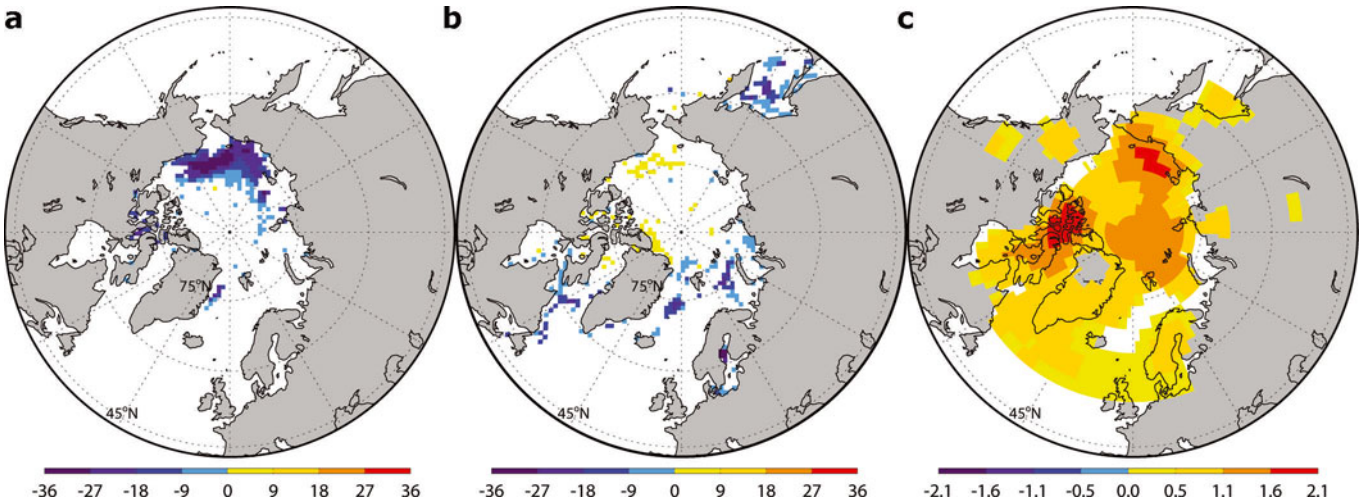

Fig. 1. Trends (1979–2006) in (a) September and (b) March sea-ice concentration, and (c) annual 925 hPa (T_{925}) air temperature. Only gridpoints with significant trends ($p = 0.05$) according to the Mann–Kendall test are shown. Units are % IC (10 a)$^{-1}$ (a, b) and °C (10 a)$^{-1}$ (c).

with isolated pockets of more rapid loss. These results are consistent with the results of others (e.g. Meier and others, 2005; Comiso, 2006) who find recent reductions in winter ice extent in both the Atlantic and Pacific sectors of the Arctic since 2002. Positive trends (~10% IC (10 a)$^{-1}$) are seen along the north coast of Greenland, in the Canadian Arctic Archipelago and in the Beaufort Sea. Trends towards increased IC north of Greenland and the Canadian Arctic Archipelago are in agreement with a recent study showing that the oldest ice is now confined to these regions (Maslanik and others, 2007b), whereas the positive winter trends in the Beaufort Sea may be related to the Beaufort Gyre, which in the past resulted in heavy, old ice moving southward into the eastern Beaufort Sea and the Canada Basin. However, since the late 1990s, multi-year ice (ice that has survived more than one melt season) has been less likely to survive the transit through the Beaufort Sea, so the trend towards higher ice concentration in the Beaufort Sea may eventually reverse direction if this pattern continues.

Over the satellite era, large increases have been reported in SATs, which are closely coupled with temperature changes at the 925 hPa level on both a seasonal and annual basis. However, details differ depending on the data source, region and time period analyzed. A study based on drifting buoys and coastal station data by Rigor and others (2000) shows positive SAT trends from 1979 to 1997 that are strongest and most widespread during spring. Analysis of surface temperature fields derived from satellites since 1981 shows pronounced warming in spring, summer and autumn (Comiso, 2003). In this study, we focus on T_{925}s from the NCEP/NCAR re-analysis, which points to larger warming in autumn than in spring and little change during summer. On an annual basis (October–September), warming is largest over the Chukchi, East Siberian and Barents seas and over the Canadian Arctic Archipelago at rates of >1.5°C (10 a)$^{-1}$ (Fig. 1c). Comparisons of Figure 1a and b with Figure 1c show that the regions with the largest annual warming trends since the late 1970s also exhibit significant decreases in sea-ice concentration during summer but not during winter. Although the large positive temperature anomalies over the Canadian Arctic Archipelago and extending into Baffin Bay do not appear to be clearly linked to ice loss, circulation variability is likely playing a role in this region. SLP fields averaged from 2003 to 2006 show positive anomalies (relative to 1979–98) of up to 4 hPa centered south of Greenland, a pattern that would help to transport warm air from the south into the region.

Arctic-wide SLP is strongly related to the AO, with positive AO values associated with lower Arctic SLP (Thompson and Wallace, 1998). The AO (not shown here) has been relatively high (i.e. Arctic SLP low) during our time domain (1979–2006) compared to the historical record back to the late 19th century. However, within our time domain, the late 1980s through mid-1990s, AO values were particularly high (strongly positive) compared to the preceding (1979–89) and subsequent (1995–2006) years (e.g. Overland and Wang, 2005; Maslanik and others, 2007a; Turner and others, 2007). There is no linear trend in the AO during our time domain, but there is significant interannual variability. Low-frequency variations in the AO, and their relationship to IC, are discussed in section 3.2.

3.2. EOF analysis

The dominant EOF modes found in the T_{925} and SLP fields reveal expected patterns of variability, and are therefore not shown here. The first mode of annual T_{925} explains 46% of the total variance. The spatial pattern of the EOF resembles the trend plot of T_{925} (Fig. 1c). When combined with the trend in the PC time series, this EOF suggests a warming trend over the entire Arctic Ocean, with largest magnitudes in the East Siberian Sea and north of Greenland. The leading mode of winter (December–March (DJFM)) SLP explains 48% of the overall SLP variability, and represents the familiar AO dipole pattern between high and mid-latitudes. The PC time series was particularly high (positive) from the late 1980s through the mid-1990s.

The spatial patterns (EOFs) of the first modes of September and March IC are represented in Figure 2a and b. The corresponding PC time series are shown in Figure 3a and b. For September IC, the leading mode explains 23% of the total variance, and the EOF mimics the spatial patterns of trends seen in Figure 1a. The first PC time series (PC1) of September IC shows a positive trend (Fig. 3a) which, when combined with the large areas of negative loadings in the spatial pattern, can be interpreted as diminishing ice concentrations throughout most of the Arctic during September. Both the

https://doi.org/10.3189/172756408784700699 Published online by Cambridge University Press

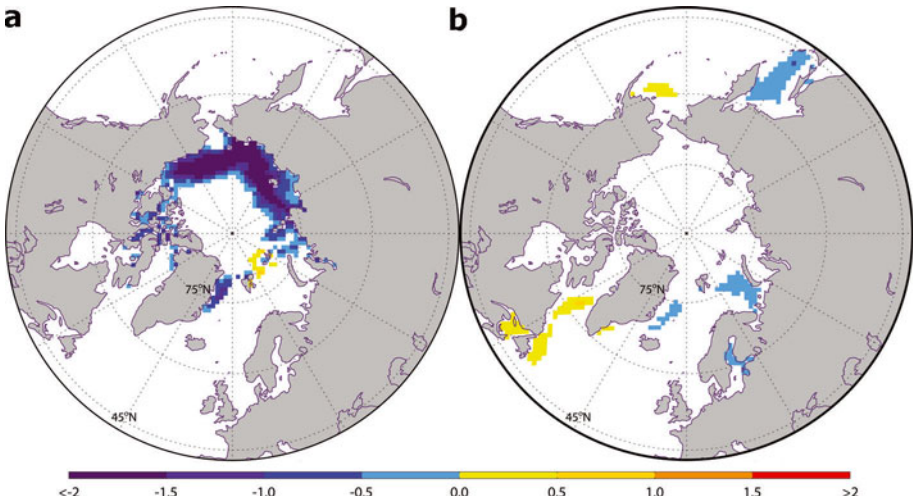

Fig. 2. Sea-ice concentration anomaly fields regressed onto the standardized PC time series for September (a) and March (b) sea-ice concentrations. Values are trends obtained by linearly regressing the sea-ice concentration anomalies onto the sea-ice concentration PC. Units are % IC a^{-1}, and values >2% a^{-1} or <–2% a^{-1} are removed.

September IC PC1 time series and annual Arctic T_{925} have increased over the satellite era (Fig. 3a), and they are significantly correlated to each other ($\rho = 0.70$). However, declining sea ice in the East Siberian Sea is also consistent with an AO-driven signal, as shown in section 3.3. Rigor and others (2002) showed that during the positive AO period there was enhanced ice transport away from the Siberian coasts (i.e. a more pronounced Transpolar Drift Stream), leading to less sea ice in this region during summer. On the other hand, the AO has decreased in recent years, while sea-ice concentrations have continued to decrease. Correlation between 9 year running means of the winter AO and the September PC1 time series indicate a weak correlation over the entire time series ($\rho = 0.39$), whereas from 1979 through 1995 the correlation is stronger ($\rho = 0.58$). This suggests a decoupling of the IC signal from the AO in later years, and that an Arctic-wide warming signal may be emerging as the more dominant factor controlling the recent September sea-ice losses.

While the second and third modes of September IC (not shown) are not well separated (they explain 13% and 12.5% of the variance, respectively), the second EOF of September IC shows a strong out-of-phase IC relationship between the western (i.e. Beaufort and Chukchi Seas) and the eastern Arctic (i.e. Laptev, Kara and Barents seas), which is consistent with the spatial pattern of summer sea-ice variability observed prior to 2002. Typically, if there was a large retreat of sea ice in the Beaufort and Chukchi Seas, there was anomalously more sea ice in the Laptev, Kara and Barents seas and vice versa. This relationship was true during the low summer sea-ice years of the 1990s (i.e. 1990, 1991, 1993, 1995 and 1998). However, this out-of-phase relationship has not been observed since 2002, despite record-breaking low IC values. Although the second EOF appears to be related to known variations in ice conditions, the proximity of the third mode makes more detailed interpretation difficult without rotation of the EOF. While the first mode may clearly relate to a physical process, the following modes are forced to be orthogonal by the statistical procedure, even if the physical mechanisms of variance are oblique (i.e. not orthogonal) (e.g. von Storch and Zwiers, 1999). The coupled nature of air temperature and atmospheric circulation suggests that the physical mechanisms that control sea-ice variations may not be orthogonal; if true, then only the first mode can be expected to reflect a distinct physical feature.

Figure 2b shows the leading March IC EOF, which explains 22% of the variance. The pattern reveals that variability in March IC is confined to the MIZ and shows an out-of-phase pattern in both the Atlantic and Pacific sectors, whereby the Barents Sea and Sea of Okhotsk vary in phase with each other, and are out of phase with the Labrador and Bering Seas. The largest negative amplitudes of the first EOF are observed in the Barents Sea and the Sea of Okhotsk, with somewhat smaller negative values in the East Greenland Sea. Positive values are not as pronounced but are present in the Labrador and Bering Seas. The PC1 time series for March sea ice indicates generally increasing values from 1979 through the early 1990s, followed by a gradual decrease through the early 2000s, with significant interannual variability superimposed (Fig. 3b).

The first mode of March IC is similar to results from Deser and others (2000) (for the years of overlap between the two analyses). One notable difference is that the signal in the East Greenland Sea is not as strong as reported by Deser and others (2000). This may be a result of the inclusion of the last three winters (2004–06), in which March sea-ice extent was anomalously low in *both* the Atlantic and Pacific sectors (corroborated by the SVD results discussed below). Correlation between March PC1 and the AO (Fig. 3b) is $\rho = 0.58$ (increasing to $\rho = 0.88$ for 9 year running means), and the spatial pattern of the correlation of March IC PC1 with DJFM SLP reveals a pattern very similar to the EOF (not shown). Our results are consistent with the interpretation by Deser and others (2000): on decadal timescales, the primary drivers for March sea-ice extent have been AO-related.

The 2 and 3 March IC modes (not shown) share a significant fraction of the total variability (14% and 11%) when compared to the first mode (22%). Neither of these two modes reflects out-of-phase sea-ice patterns as is seen in the first mode. The second PC primarily exhibits decadal-scale variability, and since 2002 has turned positive, indicating loss of ice at the margins, particularly in the Sea of Okhotsk and the Davis Strait/Labrador Sea. The third mode contains a long-term trend, representing recent loss of

https://doi.org/10.3189/172756408784700699 Published online by Cambridge University Press

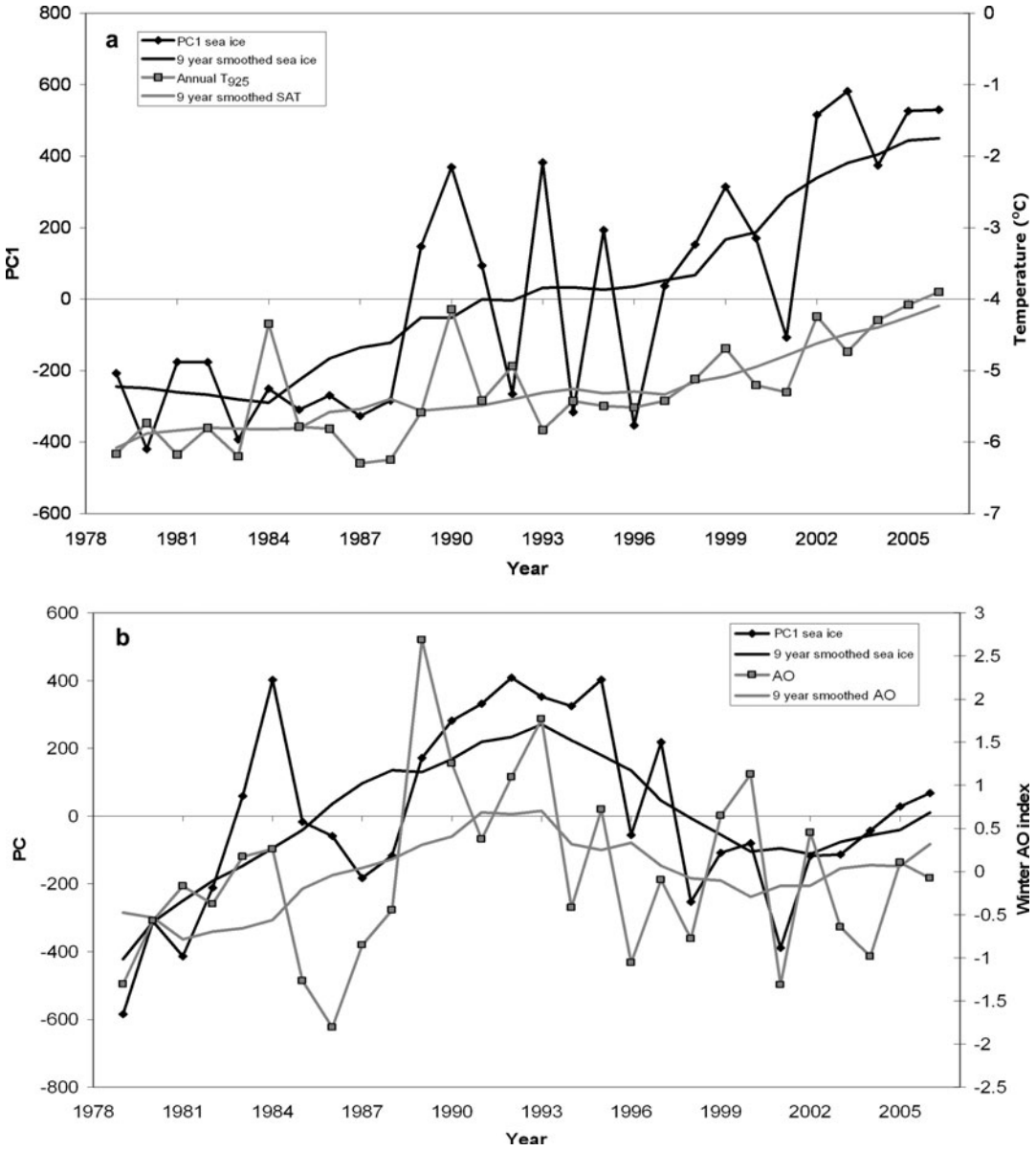

Fig. 3. Time series of (a) the first principal component (PC1) of September sea ice and Arctic annual T_{925}, and (b) PC1 of March sea ice and the winter (DJFM) AO from 1979 through 2006. Also shown are the 9 year running means.

ice in the Greenland, Barents, Labrador and Bering seas. It is suspected that the second mode is related to circulation coupled with T_{925}, while the third mode may be more directly related to the trend in T_{925}. To further understand the physical processes responsible for the second and third EOF modes, the record was divided into two non-overlapping time periods, and two independent EOF analyses were performed for 1979–94 and 1995–2006. For the pre-1995 period, the first three modes all display out-of-phase variability. In contrast, for the post-1995 period, the EOF projections are of the same sign in the MIZ, i.e. negative. While these time periods are too short to draw any definite conclusions, these results suggest that the dominant modes of variability in March IC changed during the mid-1990s.

In summary, EOF analyses show that during September a decreasing trend in sea-ice concentrations and an increasing trend in 925 hPa temperatures are the dominant modes of variability of these two fields in the Arctic. In contrast, during March, trends have not emerged as the dominant signal in IC over the entire record of observations; rather, circulation-related signals with decadal-scale temporal variations continue to explain more of the total variance. This does not mean that the winter IC deficits of recent years are unimportant, but rather that they have not been of sufficient magnitude and/or duration to emerge from the entire satellite record as a dominant mode of variability.

3.3. SVD analysis

The EOF analyses discussed above suggest potential linkages between sea ice, near-surface air temperature and the AO. These linkages could be explored further using regression analyses between T_{925}, SLP and IC PC time series. While such analyses do, in fact, support such linkages, here we demonstrate how SVD analysis can directly identify these relationships. SVD spatial patterns, time series and HC maps for the first modes are shown in Figures 4–6, respectively. A comparison of SVD (Fig. 4) and HC (Fig. 6) maps shows that in all of these analyses the SVD maps overestimate the spatial extent of significant correlations between the two fields. This is at least partly because SVD is performed on a

https://doi.org/10.3189/172756408784700699 Published online by Cambridge University Press

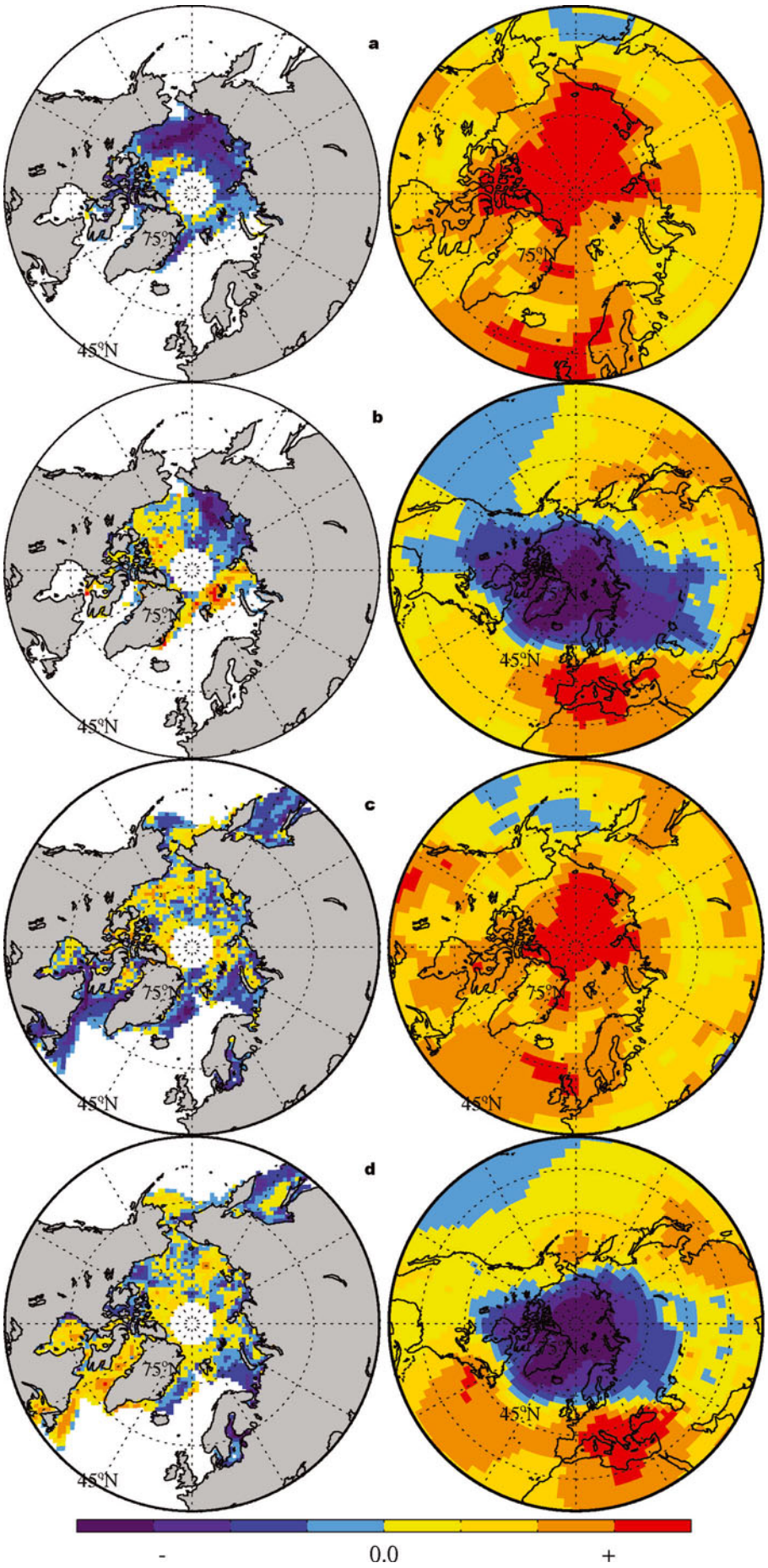

Fig. 4. SVD patterns of September and March sea-ice concentrations with annual T_{925} and winter (DJFM) SLP. (a) September sea ice and annual T_{925}; (b) September sea ice and DJFM SLP; (c) March sea ice and annual T_{925}; and (d) March sea ice and DJFM SLP. Note: units on the SVD plots are meaningless but have been normalized to range from –1 to +1.

https://doi.org/10.3189/172756408784700699 Published online by Cambridge University Press

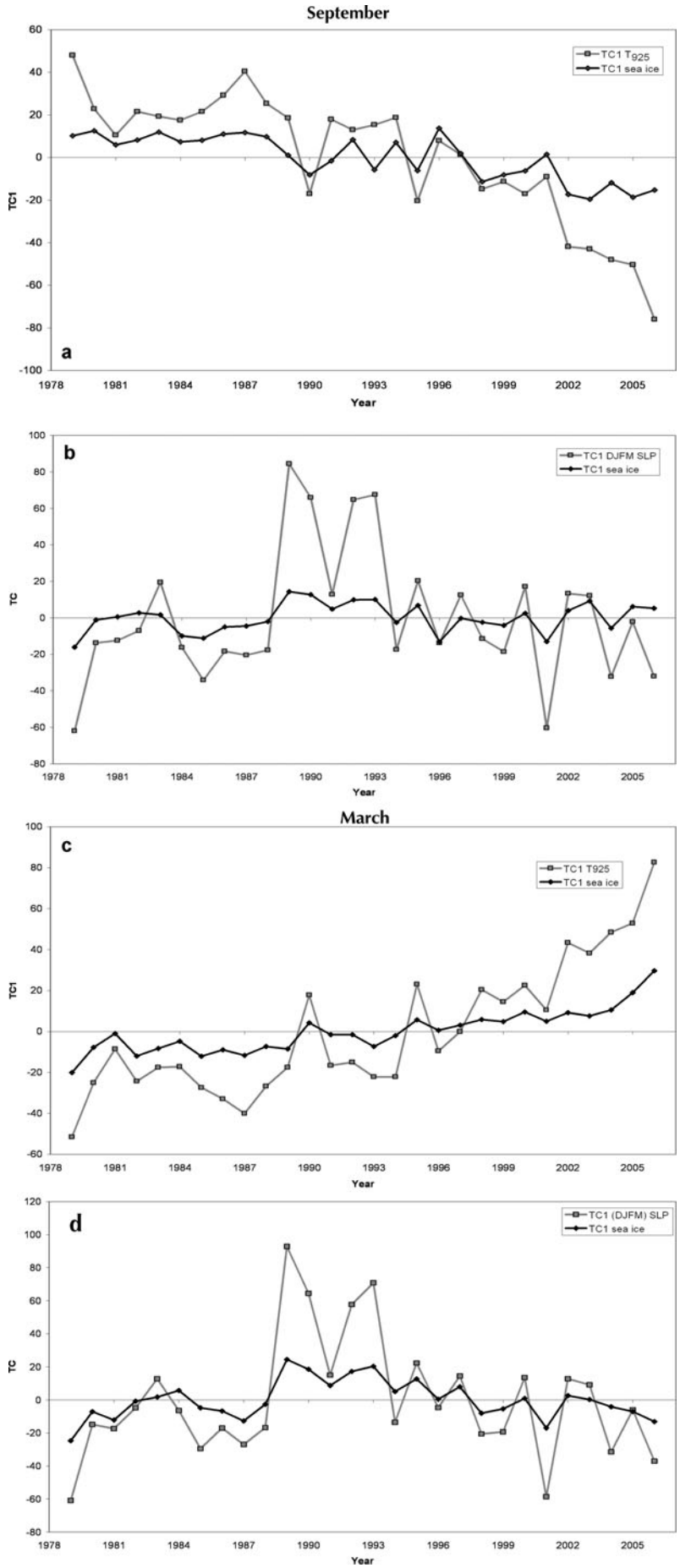

Fig. 5. Standardized time series (1979–2006) of (a) the first temporal component (TC1) of September sea ice and Arctic annual T_{925}; (b) TC1 of September sea ice and winter (DJFM) sea-level pressure (SLP); (c) TC1 of March sea ice and Arctic annual T_{925}; and (d) TC1 of March sea ice and DJFM SLP.

https://doi.org/10.3189/172756408784700699 Published online by Cambridge University Press

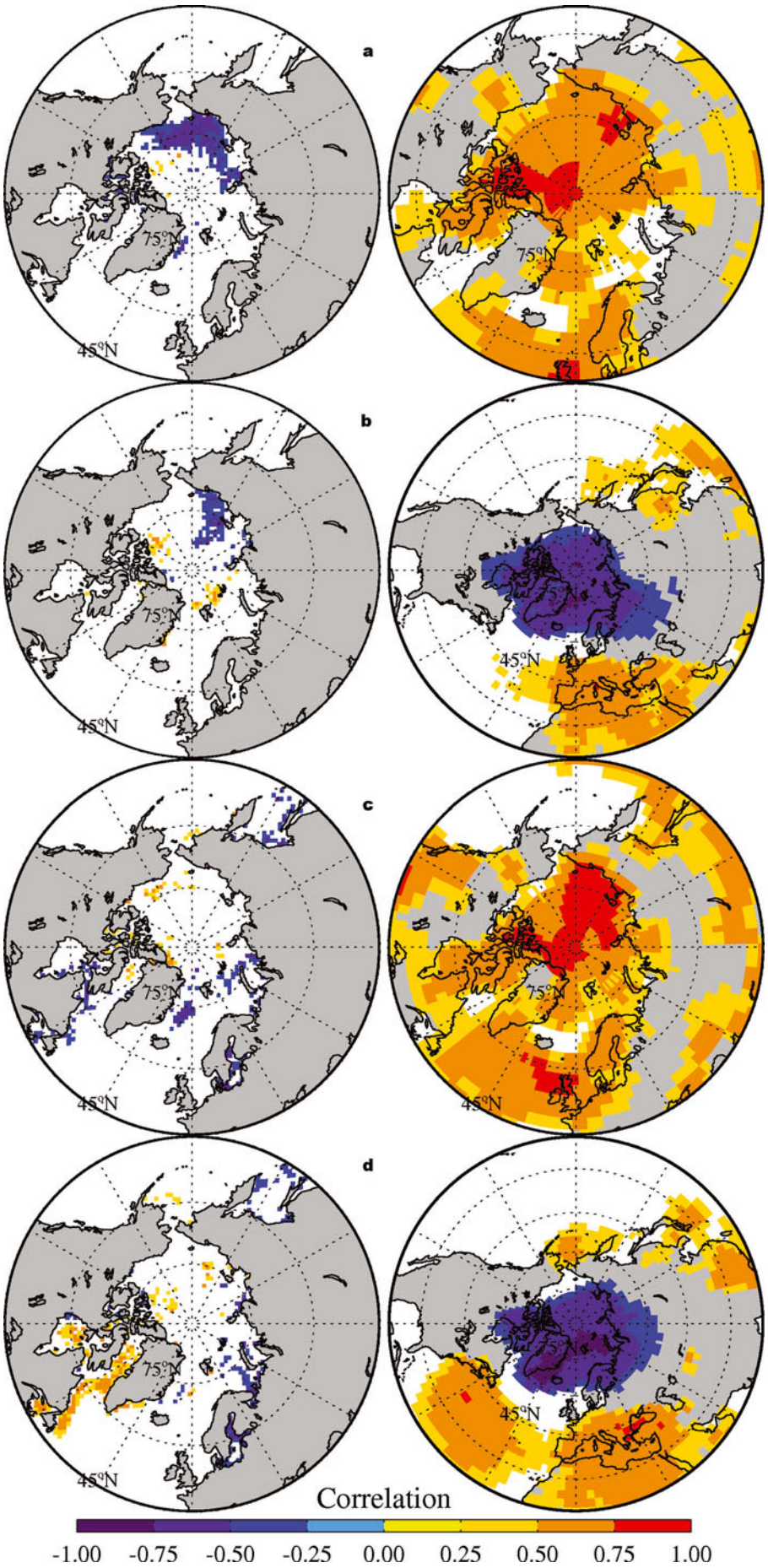

Fig. 6. Heterogeneous correlation maps (at 95% confidence) between September and March sea-ice concentrations with annual T_{925} and winter (DJFM) SLP. (a) September sea-ice concentrations and Arctic annual T_{925}; (b) September sea-ice concentrations and DJFM SLP; (c) March sea-ice concentrations and Arctic annual T_{925}; and (d) March sea-ice concentrations and DJFM SLP.

https://doi.org/10.3189/172756408784700699 Published online by Cambridge University Press

correlation basis due to disparity in the units between the fields and therefore accentuates areas of low variability. The HC maps filter out these areas of low variability, revealing where the data and the TCs are significantly correlated.

For example, the first SVD mode between September IC and annual T_{925} explains 67% of the correlation between these two fields. The spatial patterns (Fig. 4a) cover larger areas than the patterns of the first EOFs of September IC and T_{925} (Fig. 2a), although the time series (e.g. PC1 and TC1) show similar trends (Fig. 5a). The HC maps for September IC and annual T_{925} (Fig. 6a) reveal that the regions over which variations in the two fields are significantly correlated are more constrained than indicated by the SVD maps (Fig. 4a) (the HC regions are more consistent with the EOF maps of Figure 2a than with the SVD maps). Strong correlations are seen between September sea-ice variations in the Pacific sector ($-0.25 < \rho < -0.75$) and Arctic-wide T_{925} ($0.5 < \rho < 1.0$), with the most significant temperature correlations located in the East Siberian Sea and to the north of Greenland. These results suggest that the loss of sea ice in the Beaufort, Chukchi, East Siberian and Laptev seas is associated with increased T_{925} directly over those regions.

SVD results between September IC and DJFM SLP (Figs 4b, 5b and 6b) indicate sea-ice variations over the East Siberian Sea are correlated to a SLP signal (correlations in the East Siberian Sea of $-0.5 < \rho < -0.25$). The SLP signal bears the spatial pattern of the AO, which suggests that the circulation influence on summer sea ice is detectable in this analysis. However, since the trend mode was dominant in the EOF analysis, the AO is a secondary player in overall variability of September IC throughout the Arctic.

SVD results between March IC and T_{925} (Fig. 4c) indicate the first mode explains 46% of the joint variance between the two fields. The time series (Fig. 5c) indicates a trend signal associated with a warming Arctic. HC maps (Fig. 6c) confirm that the warming trend in T_{925} is related to loss of winter sea ice in the MIZ. The strong correlations in the East Greenland Sea ($-0.75 < \rho < -0.5$) are consistent with the result discussed in section 3.2, which showed a weakening of the AO signal in the East Greenland Sea. SVD reveals that the joint relationship of March IC with the trend in T_{925} is the loss of sea ice in the MIZ in a pattern that resembles both the 2 and 3 March IC EOF patterns. This provides additional support for the idea that loss of ice at the margins may be emerging in conjunction with continued increases in air temperatures in the Arctic.

The SVD and HC spatial patterns between March IC and DJFM SLP (Figs 4d and 6d) show patterns similar to the March EOF1 (Fig. 2b), which is the pattern associated with the AO: an out-of-phase relationship between the western and eastern sectors. Both the spatial pattern of DJFM SLP (Fig. 4d) and the time series for this TC1 (Fig. 5d) confirm that this is an AO-related signal. Thus, this analysis suggests that the dominant mode of the March IC is related to the AO. Further support for the influence of the AO on March IC is seen in the analysis of the second mode of SVD analysis between March ICs with T_{925}. The SVD second mode spatial pattern and the HC pattern for the sea-ice field (not shown) are similar to EOF1 for the March IC. The spatial pattern for the T_{925} field is similar to the temperature anomaly field associated with the AO (not shown), with inversely related temperature signals over eastern North America and Eurasia. Furthermore, the time series for TC2 are significantly correlated to the AO.

While these SVD analyses suggest dominance of the AO over March IC for our period of record, independent analyses of the pre-1995 and post-1995 periods (as discussed in section 3.2) reveal a change in the dominant mode of joint variability. During the earlier period we find evidence of an AO-controlled March IC field, while during the latter period a monotonic trend appears to dominate.

In summary, it appears that a trend signal has emerged in the summer sea-ice record, and that this trend is closely related to Arctic 925 hPa temperature trends. In contrast, the variability in the winter sea-ice record for the entire time period remains dominated by a circulation signal, although when analyzed independently the recent portion of the record appears to be dominated by a temperature-related trend. If recent decreases in winter ice cover continue and air temperatures continue to warm, the magnitude of the temperature-related trend signal will eventually overtake the circulation signal as the dominant mode of variability in March IC.

4. SUMMARY AND DISCUSSION

One of the difficulties in determining whether rising Arctic air temperatures are leading to diminishing sea-ice concentrations during summer and winter is related to the positive feedback between sea ice and the overlying air temperatures. As sea ice retreats (due to temperature or any other cause) and exposes the warm ocean below, air temperatures rise. Support for this 'Arctic Amplification' comes from recent analysis of a variety of SAT datasets by Serreze and Francis (2006) who conclude that we are in the early phase of Arctic Amplification. Thus, it is difficult to separate out cause and effect. The use of 925 hPa temperatures helps in this regard, but large heat fluxes to the atmosphere from the loss of sea ice still promote low-level warming at the 925 hPa level during autumn. Analysis of summer SATs, however, shows little enhanced Arctic Ocean warming. Although we only showed results using annual 925 hPa air temperatures, the conclusions reached using summer (June–August) temperatures are virtually identical to those reached using annual temperatures, which supports the conclusions reached from the multivariate statistical analysis presented here.

The AO has often been cited as a factor, in addition to temperature, in explaining reductions in September Arctic sea-ice extent. The lagged effect at seasonal timescales is attributed to the impact of AO-related winds on ice transport (Rigor and others, 2002). From the early part of this record to the mid-1990s, September IC was decreasing while the AO and Arctic air temperatures were increasing, as one might expect. Since the mid-1990s, however, September IC has continued to decrease and temperatures have continued to increase, while the AO index has reversed signs. Significant declines in sea ice continue, now statistically significant during all calendar months, with record low sea-ice concentrations and extents during the last few years (Serreze and others, 2003; Stroeve and others, 2005). This suggests that there has been a decoupling of the AO and sea ice, at least for the annual sea-ice minimum in September.

In this paper, results from trend, EOF and SVD analysis are shown to demonstrate how multivariate techniques, in particular SVD, may be used to discriminate between these different signals and better help us understand the dominant and competing physical mechanisms governing sea-ice variability in summer and winter. Summaries of the trend

https://doi.org/10.3189/172756408784700699 Published online by Cambridge University Press

Table 1. Summary of results for trend and EOF analyses. The fourth (fifth) column shows Pearson correlation coefficients between each PC and the mean annual T_{925} for the Arctic region (winter AO index). Correlations for 9 year running means are in parentheses

Field	Trend	First EOF mode	PC correlation with annual T_{925}	PC correlation with winter AO index
September sea-ice concentration	Strong decreases in the Pacific sector (up to ~35% (10 a)$^{-1}$)	Decreasing in the Pacific sector, trend mode	0.70 (0.98)	0.39 (0.41)
March sea-ice concentration	Notable decreases along the MIZ (up to ~20% (10 a)$^{-1}$)	AO-related inversely varying ice concentrations between eastern and western hemispheres	0.30 (0.16)	0.51 (0.89)
Annual air temperature	Increasing Arctic-wide	Increasing throughout Arctic basin	–0.82 (–0.90)	–0.10 (–0.18)

and EOF results are shown in Table 1. Trend analysis indicates significant decreasing trends in September IC in the Pacific sector of the Arctic basin; significant decreasing trends in March IC along the margins; and a widespread, low-level atmospheric warming trend over the entire Arctic, with the strongest signal over the East Siberian Sea and the Canadian Archipelago. EOF analysis, which identifies the dominant signals of fields when analyzed independently, shows that: (1) during September the dominant sea-ice signal is a decreasing trend in the Pacific sector; and (2) during March the dominant sea-ice signal remains AO-related when considering the entire satellite data record. However, splitting the data record into pre- and post-highly positive AO eras shows that warming may well be the dominant factor in the later years.

SVD analysis, which to our knowledge has not previously been applied to the sea-ice dataset, focused on four pairs of relationships: September and March sea-ice concentrations, both with annual 925 hPa air temperatures and with winter (DJFM) SLP. The results, summarized in Table 2, show that in September a pan-Arctic warming trend is closely related to the large-scale diminishment of sea ice in the Pacific sector; and that an apparent AO-related signal is found only over a limited region of the East Siberian Sea. Combined with the preceding EOF analysis, our SVD results indicate that the dominant mode of variability of summer sea-ice concentrations is related to Arctic-wide air-temperature trends, while the secondary mode of variability is related to the AO.

During March the trend signal dominates the covariability between March IC and T_{925}, whereas the AO signal is the dominant mode of covariance between March IC and DJFM SLP. In winter, EOF combined with SVD analysis shows that the relationship described above for summer is flipped, and the dominant mode of joint variability for winter ICs is related to the AO whereas the influence of warming air temperatures is a lesser player.

These results are consistent with combined thermal and dynamical mechanisms linking the AO to sea ice (e.g. Deser and others, 2000; Rigor and others, 2002; Lindsay and Zhang, 2005), and lead us to believe that the primary mode of variability in March sea-ice concentration remains driven by the AO, as found by Deser and others (2000), despite the fact that the AO has changed sign since the last year included in their analysis. Recent winter sea-ice deficits are of insufficient duration and/or magnitude to appear as a dominant signal in these multivariate techniques. On the other hand, contrasting results between analyses performed on pre-1995 and post-1995 observations indicate that the trend in annual air temperature has become increasingly important in recent years.

The use of SVD analysis has both advantages and drawbacks. On the one hand, it allows us to identify relationships between two fields in a concise fashion, with one set of maps and one set of time series. It also allows us to parse signals that may be confounding one another. For example, when applied to the September sea-ice and annual temperature fields as shown above, we find that the large-scale warming signal, which is dominant in the sea-ice field, exists simultaneously with an AO signal, which is more limited in its spatial domain. The SVD analysis allows us to extract these temporal signals, and their spatial patterns, from the two datasets. However, while SVD is useful for isolating combinations of variables within two fields that tend to be linearly related to one another, difficulty remains in distinguishing cause from effect. This is because these empirical analyses are based on measures of correlation or covariance, and therefore have certain limitations: they are not by themselves able to identify non-linear relationships, determine causation or identify signals associated with dynamical variations that contain significant lags due to slow response times or complicated feedbacks between different components of the climate system. Thus, the question remains: how much of the continuing trend in sea ice is forced by regional temperature trends, how much from amplification (i.e. positive albedo feedback mechanism) by the sea ice onto air temperatures, and how much

Table 2. Summary of results for SVD analyses

SVD analysis	First mode
September IC and annual T_{925}	Decreasing sea ice in the Pacific sector related to regional and Arctic-wide warming at 925 hPa
September IC and DJFM SLP	Pattern of variability mainly in the East Siberian Sea related to the AO
March IC and annual T_{925}	MIZ sea-ice loss associated with Arctic-wide warming at 925 hPa
March IC and DJFM SLP	AO-related inversely varying ice concentrations between eastern and western hemispheres

https://doi.org/10.3189/172756408784700699 Published online by Cambridge University Press

may be forced by sea-ice thermodynamics or dynamics that have multi-year lagged or non-linear effects such as suggested by Mysak and Venegas (1998) and Dukhovskoy and others (2004)?

Although the analysis presented here cannot answer those questions, other empirical evidence is consistent with the notion that air-temperature changes are responsible for a significant portion of the diminishment of Arctic sea ice (e.g. Comiso, 2003; Stroeve and others, 2006). On the other hand, other studies suggest that alternative explanations for some portion of these observed changes exist (e.g. Fowler and others, 2004; Rigor and Wallace, 2004; Francis and Hunter, 2006; Maslanik and others, 2007a). Ultimately, some combination of modeling and empirical studies that incorporate non-linear and lagged relationships must be produced that can fully explain the observed sea-ice changes in all seasons.

ACKNOWLEDGEMENTS

This paper was funded under NASA grant No. NNG04G-O51G. The sea-ice concentration data are available from the US National Snow and Ice Data Center.

REFERENCES

Bretherton, C.S., C. Smith and J.M. Wallace. 1992. An intercomparison of methods for finding coupled patterns in climate data. *J. Climate,* **5**(6), 1993–2011.

Comiso, J.C. 2003. Warming trends in the Arctic from clear satellite observations. *J. Climate,* **16**(21), 3498–3510.

Comiso, J.C. 2006. Abrupt decline in the Arctic winter sea ice cover. *Geophys. Res. Lett.,* **33**(18), L18504. (10.1029/2006GL027341.)

Deser, C., J.E. Walsh and M.S. Timlin. 2000. Arctic sea ice variability in the context of recent atmospheric circulation trends. *J. Climate,* **13**(3), 617–633.

Dukhovskoy, D.S., M.A. Johnson and A. Proshutinsky. 2004. Arctic decadal variability: an auto-oscillatory system of heat and fresh water exchange. *Geophys. Res. Lett.,* **31**(3), L03302. (10.1029/2003GL019023.)

Fowler, C., W.J. Emery and J. Maslanik. 2004. Satellite-derived evolution of Arctic sea ice age: October 1978 to March 2003. *IEEE Geosci. Remote Sens. Lett.,* **1**(2), 71–74.

Francis, J.A. and E. Hunter. 2006. New insight into the disappearing Arctic sea ice. *Eos,* **87**(46), 509.

Hu, Q. 1997. On the uniqueness of the singular value decomposition in meteorological applications. *J. Climate,* **10**(7), 1762–1766.

Huth, R. 2006. The effect of various methodological options on the detection of leading modes of sea level pressure variability. *Tellus,* **59**(1), 121–130.

Kalnay, E. *and 21 others*. 1996. The NCEP/NCAR 40-year reanalysis project. *Bull. Am. Meteorol. Soc.,* **77**(3), 437–471.

Lindsay, R.W. and J. Zhang. 2005. The thinning of Arctic sea ice, 1988–2003: have we passed a tipping point? *J. Climate,* **18**(22), 4879–4894.

Liu, J., J.A. Curry, R. Dai and R. Horton. 2007. Causes of the northern high-latitude land surface winter climate change. *Geophys. Res. Lett.,* **34**(14), L14702. (10.1029/2007GL030196.)

Mann, H.B. 1945. Nonparametric tests against trend. *Econometrica,* **13**(3), 245–259.

Maslanik, J., S. Drobot, C. Fowler, W. Emery and R. Barry. 2007a. On the Arctic climate paradox and the continuing role of atmospheric circulation in affecting sea ice conditions. *Geophys. Res. Lett.,* **34**(3), L03711. (10.1029/2006GL028269.)

Maslanik, J.A., C. Fowler, J. Stroeve, S. Drobot, H.J. Zwally, D. Yi and W. Emery. 2007b. A younger, thinner Arctic ice cover: increased potential for rapid, extensive sea ice loss. *Geophys. Res. Lett.*, **34**, L24501. (10.1029/2007/GL032043.)

Meier, W., J. Stroeve, F. Fetterer and K. Knowles. 2005. Reductions in Arctic sea ice cover no longer limited to summer. *Eos,* **86**(36), 326–327.

Mysak, L.A. and S.A. Venegas. 1998. Decadal climate oscillations in the Arctic: a new feedback loop for atmosphere–ice–ocean interactions. *Geophys. Res. Lett.,* **25**(19), 3607–3610.

Overland, J.E. and M. Wang. 2005. The Arctic climate paradox: the recent decrease of the Arctic Oscillation. *Geophys. Res. Lett.,* **32**(6), L06701. (10.1029/2004GL021752.)

Rajagopalan, B., E. Cook, U. Lall and B.K. Ray. 2000. Spatiotemporal variability of ENSO and SST teleconnections to summer drought over the United States during the twentieth century. *J. Climate,* **13**(24), 4244–4255.

Rigor, I.G. and J.M. Wallace. 2004. Variations in the age of Arctic sea-ice and summer sea-ice extent. *Geophys. Res. Lett.,* **31**(9), L09401. (10.1029/2004GL019492.)

Rigor, I.G., R.L. Colony and S. Martin. 2000. Variations in surface air temperature observations in the Arctic, 1979–97. *J. Climate,* **13**(5), 896–914.

Rigor, I.G., J.M. Wallace and R.L. Colony. 2002. Response of sea ice to the Arctic Oscillation. *J. Climate,* **15**(18), 2648–2663.

Serreze, M.C. and J.A. Francis. 2006. The Arctic amplification debate. *Climatic Change,* **76**(3–4), 241–264.

Serreze, M.C. *and 9 others*. 2003. A record minimum Arctic sea ice extent and area in 2002. *Geophys. Res. Lett.,* **30**(3), 1110. (10.1029/2002GL016406.)

Serreze, M.C., M.M. Holland and J. Stroeve. 2007. Perspectives on the Arctic's shrinking sea-ice cover. *Science,* **315**(5818), 1533–1536.

Solomon, S. *and 7 others*, eds. 2007. *Climate change 2007: the physical science basis. Contribution of Working Group I to the Fourth Assessment Report of the Intergovernmental Panel on Climate Change*. Cambridge, etc., Cambridge University Press.

Stroeve, J.C. *and 6 others*. 2005. Tracking the Arctic's shrinking ice cover: another extreme September minimum in 2004. *Geophys. Res. Lett.,* **32**(4), L04501. (10.1029/2004GL021810.)

Stroeve, J., T. Markus, W.N. Meier and J. Miller. 2006. Recent changes in the Arctic melt season. *Ann. Glaciol.,* **44**, 367–374.

Stroeve, J., M.M. Holland, W. Meier, T. Scambos and M. Serreze. 2007. Arctic sea ice decline: faster than forecast. *Geophys. Res. Lett.,* **34**(9), L09501. (10.1029/2007GL029703.)

Thompson, D.W.J. and J.W. Wallace. 1998. The Arctic Oscillation signature in the wintertime geopotential height and temperature fields. *Geophys. Res. Lett.,* **25**(9), 1297–1300.

Turner, J., J.E. Overland and J.E. Walsh. 2007. An Arctic and Antarctic perspective on recent climate change. *Int. J. Climatol.,* **27**(3), 277–293.

Von Storch, H. and F.W. Zwiers. 1999. *Statistical analysis in climate research.* Cambridge, etc., Cambridge University Press.

Zhang, X. and J.E. Walsh. 2006. Toward a seasonally ice-covered Arctic Ocean: scenarios from the IPCC AR4 model simulations. *J. Climate,* **19**(9), 1730–1747.

https://doi.org/10.3189/172756408784700699 Published online by Cambridge University Press